Bull. Korean Fish. Soc. 20(6), 477~483, 1987 韓水誌 20(6), 477~483, 1987

Objective Interpolation of the M_2 Tide in the East Sea*

Yong Q. KANG and Seog-Won CHOI
[Department of Oceanography, National Fisheries University of Pusan, Pusan, 608 Korea
(Received September 2, 1987; Accepted November 11, 1987)

We constructed the tidal chart of M_2 tide in the East Sea (Japan Sea) by an objective method. The sea level elevations at coastal stations are specified as Dirichlet boundary conditions, and the tidal constants inside of the East Sea basin are determined by the solution of the complex partial differential equation for the sea surface elevation. We studied the influences of the bottom topography and the tidal friction on the distribution of tidal chart inside of the basin. Using the results of basin-wide tidal model, we constructed a detailed tidal chart of the M_2 tide off east of Korea.

Introduction

Tidal currents and tide-associated surface elevations are described by the Laplace tidal equation. An analytic solution for the Laplace tidal equation, with a consideration of actual bottom topography and coastal geometry, is practically impossible. Quantitative studies on tides in actual situations are usually made by numerical simulation techniques using finite difference method or finite element method. In the numerical simulations, one usually specifies the sea surface elevation at the open-sea boundaries and applies a vanishing normal flow condition at coastal boundaries. In addition to the requirement of a large computer time, the numerical simulation technique has another disadvantage that the observed tidal constants at coastal stations are not directly entered in the simulation.

The harmonic method of tide is a powerful and simple method in studying tides in the ocean, provided the tidal observations at coasts are sufficient to specify boundary conditions. In the harmonic method, the tide-associated currents and sea surface elevations are assumed to vary sinusoidally in time. In this case, as will be shown later, one can obtain a complex partial differential equation for the sea surface elevation, and the tidal constants inside of the basin are determined by the solution of the boundary value problem. The tidal currents can be computed from the informations of the surface elevation. The harmonic method has advantages that it requries only a small computer time and the observed tidal constants at coasts are directly used as boundary conditions.

The tidal charts for major constitutents of tides in the neighbouring seas of Japan, including the East Sea, were made by Ogura (1933). Ogura's tidal charts, which are based on the harmonic constants at coasts, involved considerably subjective decisions. The tidal charts in the same region were later improved by Nishida (1980), but he did not state the method by which he constructed the tidal charts.

In this paper we present an objective method to construct tidal charts using tidal constants at coasts. The tidal charts are made by the solution of the Dirichlet boundary value problem for the sea surface elevation. We examine the effects of bottom topography and the friction on the distribution of tidal characteristics inside of the basin.

A knowledge on the tidal constants inside of the basin are essential for modelling tidal phenomena in a localized small area. Using the results of the

* 이 논문은 한국학술진흥재단의 1986년도 연구비에 의하여 연구되었음.
Contribution No. 192 of Institute of Marine Sciences, National Fisheries University of Pusan, Korea.

basin-wide model as boundary conditions for the local tide model, we constructed a local tidal chart for the M_2 tide off east coast of Korea at fine grids with a mesh size of 6.9 km.

Tidal Computation

1. Governing Equations

The linearized tidal equations of momentum and continuity in an f-plane ocean are

$$\begin{aligned}&\frac{\partial u}{\partial t}-fv=-g\frac{\partial \zeta}{\partial x}-ru\\&\frac{\partial v}{\partial t}+fu=-g\frac{\partial \zeta}{\partial y}-rv\\&\frac{\partial \zeta}{\partial t}+\frac{\partial}{\partial x}(Hu)+\frac{\partial}{\partial y}(Hv)=0,\end{aligned}\tag{1}$$

where t is the time, u and v are the barotropic velocities to the x (eastward) and y (northward) directions, respectively, $\zeta(x, y, t)$ is the sea surface elevation, f is the Coriolis parameter, g is the gravity, r is a linear friction coefficient, and $H(x, y)$ is the depth of the ocean.

We assume that u, v and ζ vary sinusoidall in time. That is,

$$\begin{aligned}u(x, y, t)&=U(x, y)\ \exp(i\omega t)\\v(x, y, t)&=V(x, y)\ \exp(i\omega t)\\\zeta(x, y, t)&=Z(x, y)\ \exp(i\omega t),\end{aligned}\tag{2}$$

were ω is the angular frequency of tidal motion, and U, V and Z are complex amplitudes. By using (2), the equations (1) become

$$\begin{aligned}&(i\omega+r)U-fV=-g\frac{\partial Z}{\partial x}\\&fU+(i\omega+r)V=-g\frac{\partial Z}{\partial y}\\&i\omega Z+\frac{\partial}{\partial x}(HU)+\frac{\partial}{\partial y}(HV)=0.\end{aligned}\tag{3}$$

From the first two equations of (3) we get

$$\begin{aligned}U&=-g\frac{(i\omega+r)\frac{\partial Z}{\partial x}+f\frac{\partial Z}{\partial y}}{(i\omega+r)^2+f^2}\\V&=-g\frac{(i\omega+r)\frac{\partial Z}{\partial y}-f\frac{\partial Z}{\partial x}}{(i\omega+r)^2+f^2}.\end{aligned}\tag{4}$$

By susbstituting U and V into the third equation of (3), we get a partial differental equation for Z only:

$$\begin{aligned}&\frac{\partial}{\partial x}\left(H\frac{\partial Z}{\partial x}\right)+\frac{\partial}{\partial y}\left(H\frac{\partial Z}{\partial y}\right)+A\left(\frac{\partial H}{\partial x}\frac{\partial Z}{\partial y}\right.\\&\left.-\frac{\partial H}{\partial y}\frac{\partial Z}{\partial x}\right)+BZ=0,\end{aligned}\tag{5}$$

where A and B are constants defined by

$$\begin{aligned}A&=\frac{f}{i\omega+r}\\B&=-\frac{i\omega}{g}\frac{(i\omega+r)^2+f^2}{i\omega+r}.\end{aligned}\tag{6}$$

When the values of Z at coasts are specified as Dirichlet boundary conditions, the values of Z inside of the basin can be determined by the solution of (5).

2. Numerical Method

The surface elevation equation, (5), is approximated by the finite difference method. Employing the central difference method for the derivatives of elevations and depths, and using the "star-5" rule for the Laplacian operator, the elevation Z at (i, j)-th grid is represented in terms of elevations at surrounding grids by

$$aZ_{i,j}=bZ_{i-1,j}+cZ_{i+1,j}+dZ_{i,j+1}+eZ_{i,j-1}\tag{7}$$

where subscripts i and j are grid numbers in x- and y-directions, respectively, and a, b, c, d and e are multipliers given by

$$\begin{aligned}a&=2(4H-D^2B)&&\text{(center grid)}\\b&=2H-DF+ADG&&\text{(left grid)}\\c&=2H+DF-ADG&&\text{(right grid)}\\d&=2H+DG+ADF&&\text{(upper grid)}\\e&=2H-DG-ADF&&\text{(lower grid).}\end{aligned}\tag{8}$$

In (8), D is a grid spacing, $F=\partial H/\partial x$, and $G=\partial H/\partial y$. Since the depth and its derivatives differ from grid to grid, the values of multiplier in (8) differ from grid to grid.

The values of Z at interior grids can be found by the iteration of (7). However, more efficient convergence is achieved by the successive over-relaxation (SOR) method (Gerald and Wheatley, 1984). The SOR iteration formula corrsponding to (7) is

$$\begin{aligned}Z_{i,j}^{(k+1)}=Z_{i,j}^{(k)}+\frac{p}{a}(&bZ_{i-1,j}+cZ_{i+1,j}+dZ_{i,j+1}\\&+eZ_{i,j-1}-aZ_{i,j})^{(k)}\end{aligned}\tag{9}$$

where superscripts (k) and $(k+1)$ represent the

iteration steps, and p is a relaxation factor.

3. Tidal Chart from complex Amplitudes

From the complex amplitude of elevation, the co-tidal and co-amplitude lines can be computed as follows. The sea surface elevation, $\zeta(x, y, t)$, can be expressed as

$$\zeta(x, y, t) = Z(x, y)\exp(i\omega t)$$
$$= |Z(x, y)|\exp[i(\omega t - \phi(x, y))], \quad (10)$$

where

$$|Z(x, y)| = (Z_r^2 + Z_i^2)^{1/2} \quad (11)$$
$$\phi(x, y) = \tan^{-1}(-Z_i/Z_r),$$

In (11), Z_r and Z_i are the real and imaginary parts of $Z(x, y)$, respectively. Co-amplitude lines are constructed by following lines along which $|Z(x, y)|$ is constant. Co-tidal lines are described by curves along which $\omega t - \phi(x, y) = \text{constant}$, or

$$t(x, y) = \phi(x, y)/\omega + \text{constant}. \quad (12)$$

4. Grid Scheme and Data

Tidal computations in the East Sea are made at rectangular grids shown in Fig. 1. The grid spacings are 1/3 degree in longitude and 1/4 degree in latitude. We choose the reference latitude at 42°N, and the grid spacings in both x- and y-directions are 27.5 km.

The amplitudes and phases at boundary grids (open circles in Fig. 1) are interpolated from the tidal constants at coastal stations (Ogura 1933, Choi 1980). The complex amplitudes at interior grids

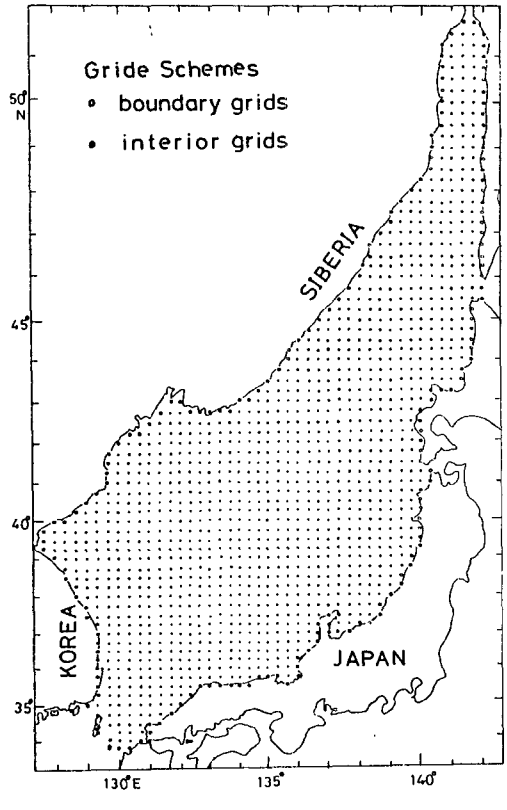

Fig. 1. Rectangular grids used in tidal computation of the East Sea. Open circles denote boundary grids and dots denote internal grids.

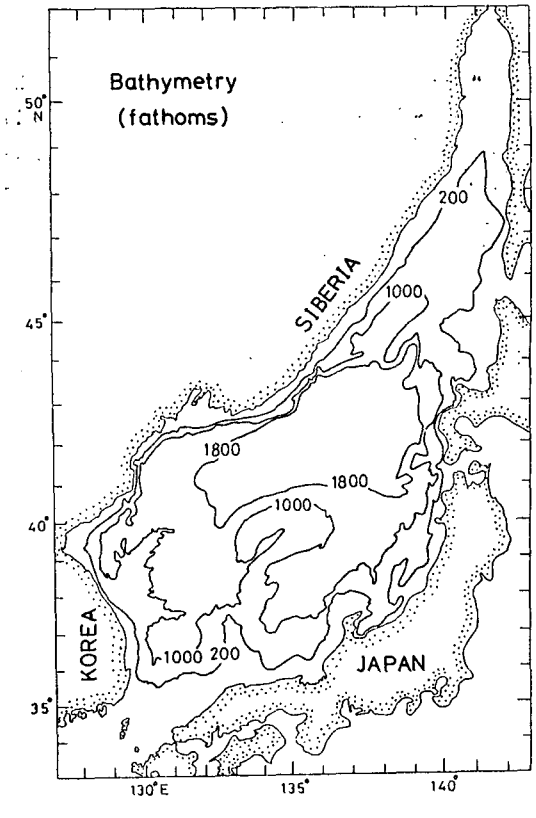

Fig. 2. Bathymetry of the East Sea. Depths in fathoms.

dots in Fig. 1) are computed by the SOR method discussed above.

The data for the bottom topography at each grid are read from a bathymetric atlas (Menard and Chase, 1973). Fig. 2 shows a crude bathymetry of the East Sea.

Tidal Charts

We studied the influences of the bottom topography and the friction on the internal distribution of tide in the East Sea. The effect of bottom topography is studied by comparing the M_2 tidal chart in a flat bottom basin and that in the basin with the actual bottom topography. The effect of friction is studied by constructing tidal charts associated with various values of friction coefficient.

1. Effect of Bottom Topography

The M_2 tidal charts in the East Sea for the cases of a uniform depth of 1000 m is shown in Fig. 3 and that for the case of actual topography is shown in Fig. 4. In both cases, the boundary values used are the same and the friction is assumed to be zero. The cotidal lines are in units of lunar hour with respect to the moon's passage across 135°E meridional, and the co-amplitude lines are drawn at every 10 cm interval, except the contour of 5 cm at the vicinity of the amphidromic points. In both cases, there appear two amphidromic points in the East Sea.

The bottom topography gives a considrable change in the location of the amphidromic point in the southern part. The southern amphidromic point for the case of actual topography is located closer to Japan than that for the case of flat bottom. The northern amphidromic point for the case of actual topography is located slightly closer to Siberian coast than that for the case of flat bottom.

The bottom topography gives a significant change for the M_2 tide in the central part of the East Sea. For the case of flat bottom, the cotidal line of lunar hour 3 connects the Siberia and Japan across the central portion of the basin (Fig. 3).

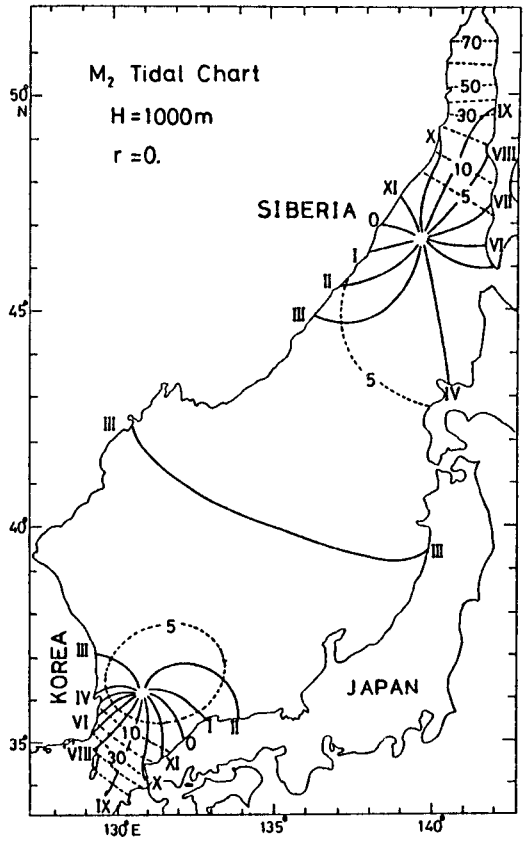

Fig. 3. The M_2 tidal chart of the East Sea for the case of a constant depth of 1000 *m* and no friction. Cotidal lines are in lunar hours and co-amplitudes are in *cm*.

But for the case of actual topography, the cotidal line of lunar hour 3 passes along the Korean and Japanese coasts.

2. Effect of Friction

Figs. 4, 5 and 6 show the M_2 tidal charts in the East Sea with three different values of friction coefficients: 0, 0.97×10^{-5} sec^{-1} ($=f/10$), and 9.7×10^{-5} sec^{-1} ($=f$), respectively, where f is the Coriolis parameter. In all of the three cases, we considered the basin with the actual bottom topography. Figs. 4, 5 and 6 show that, with an increase of the friction coefficient, the amphidromic point in the northern part moves toward Siberian coast and that in the southern part moves toward Japanese coast. However, there is almost no appreciable difference between the tidal chart

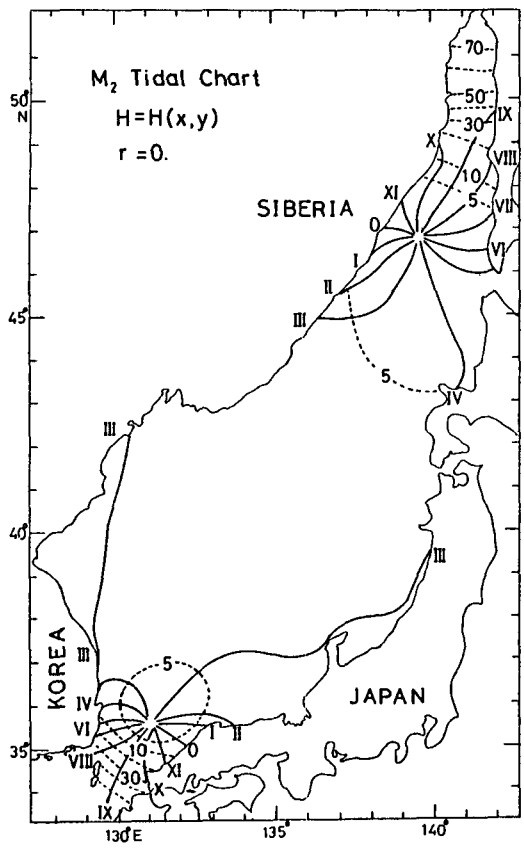

Fig. 4. The M_2 tidal chart of the East Sea for the case of actual bottom topograph and no friction.

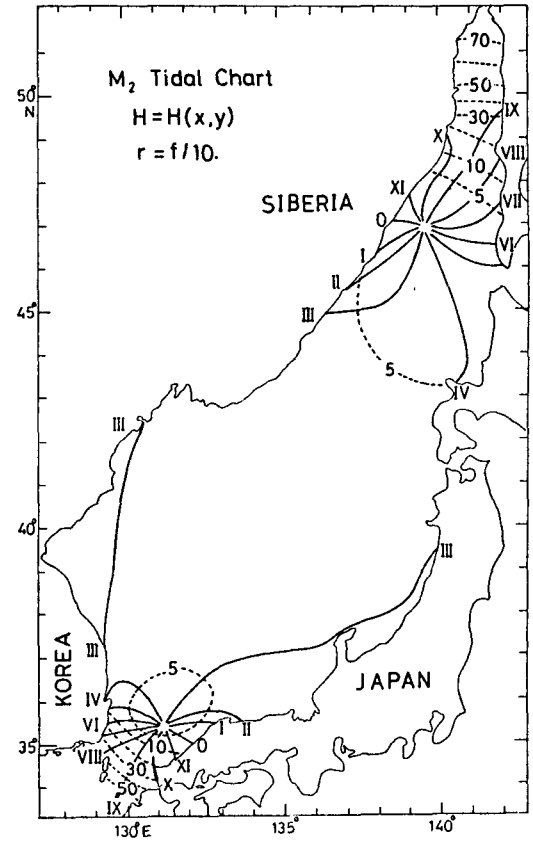

Fig. 5. The M_2 tidal chart of the East Sea for the case of actual bottom topography and a friction coefficient $r=f/10$.

for the case of no friction (Fig. 4) and that for the case with a reasonable friction coefficient of f/10 (Fig. 5). This shows that the friction plays only a minor role in the distribution of tidal behavior inside of the basin.

3. Local Tidal Chart

We made a detail M_2 tidal chart of the southwestern East Sea (33.9−38.8°N, 128.2−132.0°E). The grid distances are 1/12 degree in longitude (6.9 km) and 1/16 degree in latitude (6.9 km). The amplituds and phases of elevation along Korean and Japanese coasts are interpolated from the observed harmonic constants at coastal stations (Ogura 1933, Choi 1980), and those along the open-sea boundary grids are interpolated from the results of the basin-wide model (Fig. 5). The linear friction coefficient is assumed to be 0.97×10^{-5} sec^{-1} ($=f/10$).

According to the local tidal chart, shown in Fig. 7, the M_2 tide in the southwestern part of the East Sea are characterized wich an amphidromic system rotating counterclockwise around the amphidromic point. The amplitudes are large in the Korea Strait and small in the northern part.

Discussion and Conclusions

In this paper, based on an objective method to construct tidal chart, we studied the influences of the bottom topography and the tidal friction on the distributions of amplitude and phase of M_2 tide inside of the East Sea. We compare our results with a previous M_2 tidal chart by Nishida (1980), which is shown in Fig. 8.

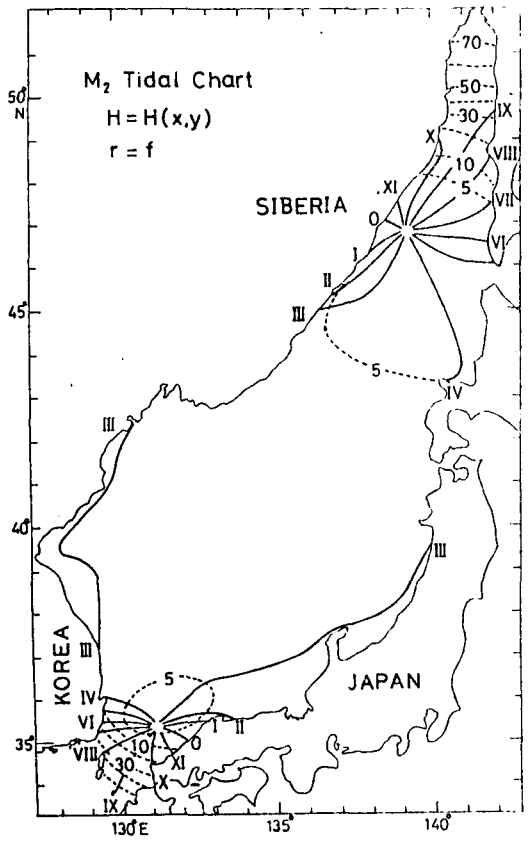

Fig. 6. The M_2 tidal chart of the East Sea for the case of actual bottom topography and a friction coefficient $r=f$.

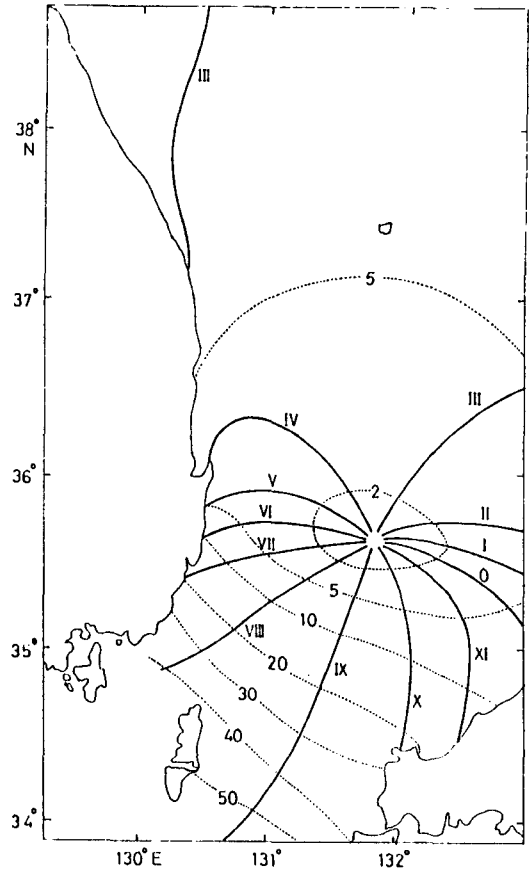

Fig. 7. The M_2 tidal chart off east coast of Korea, for the case of actual bottom topography and a friction coefficient $r=f/10$, computed at fine grids with mesh size of 6.9 *km*.

Our results (Fig. 3, 4, 5 and 6) show that the amphidromic points in the southern part of the East Sea is located closer to Japan than that by Nishida (Fig. 8). In the Nishida's chart, there appears a cotidal line of lunar hours 3 (phase angle 90°) connecting Siberia and Japan directly across the central part of the basin. In our case, the cotidal line of lunar hour 3 in the central of the basin appears only for the case of hypothetical basin with a constant depth of 1000 *m* (Fig. 3). When the actual bottom topography is considered, the cotidal line of lunar hour 3 does not directly connect Siberian and Japanese coasts across the central part of the basin (Fig. 4, 5 and 6).

The computed phase, 96°, at Ullungdo (37°30'N, 130°55'E) agrees exactly with the observed phase, 91°. But the computed amplitude of 5.7 *cm* at Ullungdo is larger than the observed amplitude of 4 *cm* (Uda, 1933). The reason for the discrepancy between the computed and observed amplitudes is not clear.

The distributions of cotidal and co-amplitude lines inside of East Sea, associated with the same boundary conditions at coast, depend on bottom topography and tidal friction. Compared to the case of flat bottom, the amphidromic points in the northern and southern part for the case of actual topography are located closer to Siberia and Japanese coasts, respectively. With an increase of tidal friction, the northern and southern amphidromic points move slightly toward Siberian and Japanese coasts, respectively.

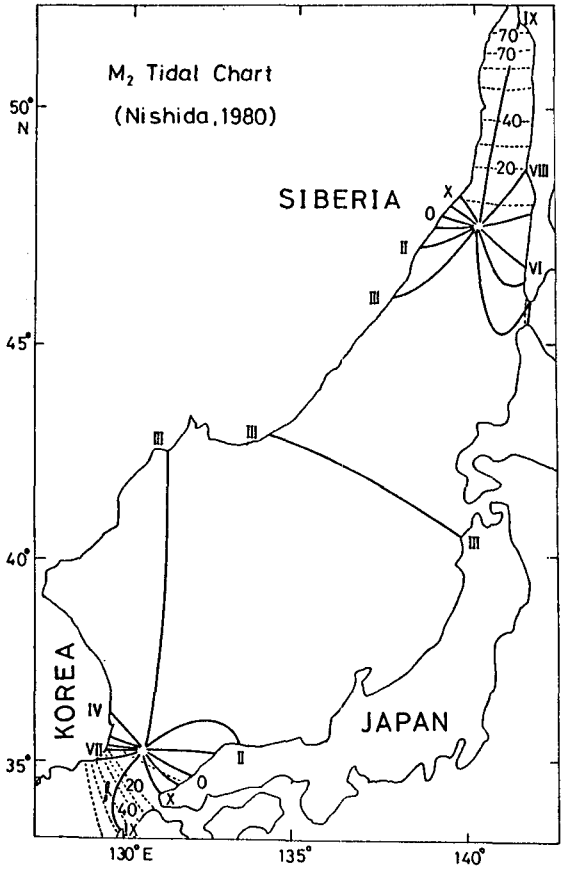

Fig. 8. M_2 tidal chart of the East Sea drawn by Nishida (1980).

Acknowledgments

This work is carried out as a part of "The Study on the Tides in the East Sea", which was supported by the Korea Research Foundation. The Computer Center of the National Fisheries University of Pusan provided computer time and facilities for this work. We thank Dr. Hee Joon Km, National Fisheries University of Pusain, for his careful reading of the manuscript and helpful comments.

References

Choi, B. H. 1980. A Tidal Model of the Yellow Sea and the East China Sea. p. 72. Korea Ocean Research and Development Institute. Seoul. Rep. No. 80—02.

Gerald, C. F. and P. O. Wheatley, 1984. Applied Numerical Analysis. 3rd Edition. p. 579. Addison-Wesley Publ. Co.

Menard, H. W. and T. E. Chase, 1973. Bathymetric Atlas of the North Pacific Ocean. p. 172. U. S. Naval Office, Publ. No. 1301-2-3. Washington, D. C.

Nishida, H. 1980. Improved tidal charts for the western part of the North Pacific Ocean. Rep. Hydrogr. Res. (Tokyo) 15, 55—70.

Ogura, S. 1933. The tides in the seas adjacent to Japan. Hydrogr. Bull. Dep. Imp. Jap. Navy 7, 1—189.

객관적 방법에 의한 동해의 반일주조 조석도

강 용 균·최 석 원
부산수산대학 해양학과

조석방정식에 근거한 객관적 방법으로 동해내 반일주조(M_2조)의 조석도를 작성하였다. 조석도의 작성은 라프라스 조석방정식으로부터 유도된 해면변위 방정식의 해로서 구하였으며, 이때 연안 검조소에서 관측된 해면변위의 진폭과 위상을 경계조건으로 사용하였다. 본 연구에서는 동해의 해저 지형과 조류에 따른 마찰력이 동해의 조석도 분포에 미치는 영향을 구명하였다. 또한, 동해 전역의 조석도의 결과를 기초로 하여, 한반도 동해안 외해의 국지적 영역의 반일주조에 대한 정밀조석도를 작성하였다.